



OPEN

Combining humic acid with phosphate fertilizer affects humic acid structure and its stimulating efficacy on the growth and nutrient uptake of maize seedlings

Jianyuan Jing¹, Shuiqin Zhang¹, Liang Yuan¹, Yanting Li¹, Zhian Lin¹, Qizhong Xiong² & Bingqiang Zhao¹✉

This paper analyzed the compositional and structural changes of humic acid (HA) after combined with phosphate fertilizer (PHA), and investigated its effects on the growth of maize seedlings with four humic acid concentrations. The results showed that the atomic ratios of O/C and (O + N)/N of PHA were significantly lower than those of HA, which indicated that PHA had poor hydrophilicity compared with HA. The spectra of FTIR and NMR results suggested that the relative content of carboxyl group in PHA was higher than that in HA. X-ray photoelectron spectroscopy technology showed that the relative amount of C–C in PHA was lower than that in HA, while C–H was the opposite. The above changes were attributed to the crack of HA structure during the preparation of humic acid enhanced phosphate fertilizer, which was verified by the results from the determination of gel permeation chromatography that there were more low molecular weight components in PHA than that in HA. However, compared with HA, PHA showed a worse effect in promoting growth and the uptake of nitrogen, phosphorus and potassium by maize seedlings. This worse effect might be attributed to the poor hydrophilicity and unsuitable addition amount of PHA.

Humic acid is an organic compound derived from plant and animal residues and microbial cells with long-term physical, chemical, and biological processes, and it is also a natural material that improves the efficiency of phosphate fertilizers¹. Many studies have shown that humic acid co-applied with monocalcium phosphate can increase the movement and availability of P in soil^{2,3}. Furthermore, humic acid can enhance the efficiency of phosphate fertilizers by promoting H⁺ release in the rhizosphere and increasing phosphate uptake by plants^{4–6}. However, in the above studies, humic acid is always applied to the soil in large amounts.

In recent years, conventional phosphate fertilizers combined with trace amounts of plant-based biostimulants have become an emerging way to improve the efficiency of phosphate fertilizers, and the manufactured fertilizer is called value-added phosphate fertilizer^{7,8}. It shows a distinct advantage based on its large output and low cost. Humic acid is often used in the process of making value-added phosphate fertilizers, and the corresponding product is called humic acid enhanced phosphate fertilizer (HAP), the yield of which reached 500,000 tons in China in 2019.

Field studies have reported that HAP showed a better performance in crop yield and apparent phosphate utilization than common phosphate fertilizers^{7,9,10}. One possibility is that the application of HAP reduced the soil pH, increased the available phosphorus content in the soil, and promoted the uptake of phosphorus by plants^{8,10}. At the same time, it may be closely related to the formation of bioavailable phosphate nanoparticles stabilized by the etching of phosphate crystals³. Humic acid could convert insoluble phosphorus into dissolved phosphorus

¹Key Laboratory of Plant Nutrition and Fertilizer, Ministry of Agriculture and Rural Affairs / Institute of Agricultural Resources and Regional Planning, Chinese Academy of Agricultural Sciences, Beijing 100081, China. ²Anhui Province Key Laboratory of Farmland Ecological Conservation and Pollution Prevention, School of Resources and Environment, Anhui Agricultural University, Hefei 230036, China. ✉email: zhaobingqiang@caas.cn

Sample	Elemental composition (%)					Ash content (%)	Atomic ratios			
	C	H	O	N	S		H/C	O/C	N/C	(O + N)/N
HA	59.48 ^a	2.74 ^a	31.08 ^a	2.54 ^b	0.75 ^a	3.40 ^a	0.55 ^a	0.39 ^a	0.04 ^b	11.86 ^a
PHA	59.36 ^a	2.76 ^a	29.16 ^b	5.70 ^a	0.67 ^a	2.35 ^b	0.56 ^a	0.37 ^b	0.08 ^a	5.59 ^b

Table 1. Elemental composition and atomic ratio of the HA and PHA. HA humic acids, PHA humic acids extracted from humic acid enhanced phosphate fertilizer. Means with no letter in common are significantly different ($P < 0.05$), as indicated by the least significant difference (LSD) test ($n = 3$).

due to the ion exchange with anions of humic acid and remineralization into more soluble phosphorus^{11,12}. In addition, humic acid was also used as phosphorus recycled material and then to stimulate plant growth^{13,14}. However, researchers have paid almost all attention to the effect of HAP on the availability and utilization of phosphorus fertilizers, and they have ignored the possibility that the combination with phosphate fertilizers might change the structure and function of humic acid.

During the production process of chemical phosphate fertilizers, the exothermic neutralization reaction of phosphoric acid and alkaline substances occurs, and a high temperature is generated^{15,16}. The changed temperature may affect the structure of humic acid. When the temperature of the reaction system reaches 290 °C, the elemental content and atomic ratio of humic acid will change¹⁷. Zhang et al.¹⁸ reported that high temperatures (> 400 °C) will also cause a serious loss of humic acid by weight, especially for aliphatic compounds. Zhou et al.¹⁹ also reported that the temperature of the reaction system is the most important factor affecting the properties of humic acids. However, the effect of the high temperature generated during the production process of HAP on the structure of humic acid has not been reported.

The structural variation of humic acid will also change its biological activity. Compared with raw humic acid, oxidized humic acid with a high yield of small molecular weight, low aromaticity, and low hydrophobicity index can significantly improve the root biomass and activity of maize²⁰. By comparing four humic acids from different sources, Jindo et al.²¹ found that humic acid with more carboxylic groups and a high hydrophobicity can promote the growth of the maize root system. García et al.²² also reported that humic acid with more labile and functionalized groups is responsible for root emission, while that with more recalcitrant and less functionalized groups is related to root growth. Furthermore, the effect of humic acid on the nutrient uptake of plants is also related to its structure. Albuizio et al.²³ reported that fractionated humic acids will significantly reduce the nitrate uptake of barley, while the content and type of functional groups of humic acid will be changed after fractionating²⁴.

Therefore, we extract humic acid from HAP (PHA) by adjusting the pH of the HAP solution. The objective was to study the changes in the structure of humic acid after combining with phosphate fertilizer and the effects on the growth and nutrient uptake of maize seedlings. The structures of raw humic acid (HA) and PHA were determined by various characterization techniques, and the effects of HA and PHA on the growth and nutrient uptake of maize seedlings were investigated via hydroponic experiments with four concentrations. This research could explain the synergistic mechanism of HAP.

Results and discussion

Characterization of HA and PHA. The elemental compositions of HA and PHA are shown in Table 1. HA and PHA exhibited a significant variation in the contents of oxygen, nitrogen, and ash and in the atomic ratios of O/C, N/C and (O + N)/N. Carbon was the main component, accounting for 59.48% and 59.36% of the HA and PHA, respectively, which was consistent with the results of Zhang et al.²⁴. Compared with HA, the ash contents of PHA significantly decreased by 30.88% ($P < 0.05$), while the nitrogen content significantly increased by 124.41% ($P < 0.05$). The decrease of the ash content in PHA indicated the loss of inorganic components, which might be attributed to the removal of soluble metal ions during the PHA extraction process. There were no nitrogenous substances involved in the production of HAP, but the nitrogen content showed an obvious increase, which might be related to the change of the other components of the PHA, such as the decrease of ash contents.

In addition, the hydrophobicity of humic acid had a negative correlation with the relative atomic number of O²⁵. Our results showed that atomic ratios of O/C and (O + N)/N of PHA were significantly lower than those of HA, which indicated that PHA had poor hydrophilicity compared with HA.

The surface morphologies of HA and PHA are shown in Fig. 1a–d. There was no significant difference between PHA and HA, and both of them exhibited a loose and abundant structure with nonhomogeneous pores. This outcome indicated that after combination with phosphate fertilizer, the amorphous structure of humic acid was well-maintained¹⁷.

The FTIR spectra of HA and PHA are shown in Fig. 2a, and the relative absorption intensity of the main absorption peaks is listed in Table S1 (see Supplementary Table S1 online). PHA showed a similar FTIR spectrum to HA. The peaks at 3418 and 3415 cm^{-1} were attributed to –OH stretching in alcohols and phenols. The stretching vibration of carboxyl group C=O was found at 1707 and 1709 cm^{-1} and the C–O–H in-plane bending vibration of carboxylic acid at 1421 and 1417 cm^{-1} ^{17,19}. According to the integration in Table S1 (see Supplementary Table S1 online), the vibration intensity of the above functional groups in HA was weaker than that in PHA, which indicated that the relative carboxyl content of PHA was higher than that of HA. In addition, compared with HA, the vibration intensity of PHA at 900–600 cm^{-1} decreased (see Supplementary Table S1 online), which indicated that the ash in the PHA was reduced, similar with the result of the elemental composition (Table 1).

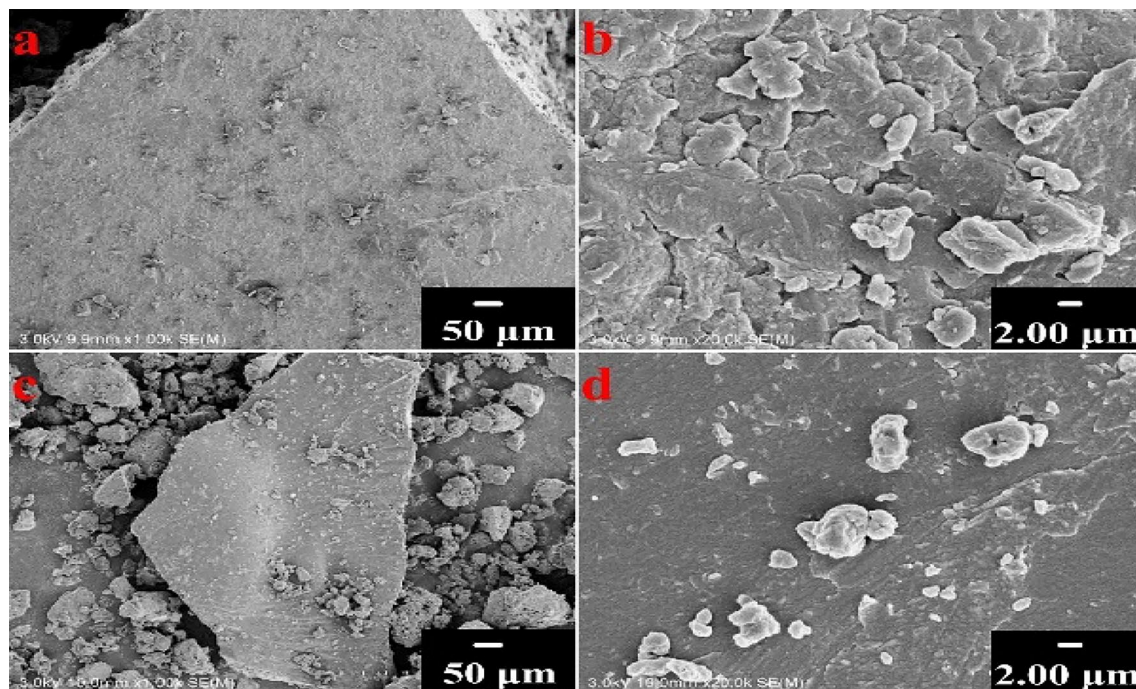


Figure 1. SEM images of HA and PHA. **a,b** for HA with magnified 1000 and 20,000 times, respectively; **c,d** for PHA with magnified 1000 and 20,000 times, respectively.

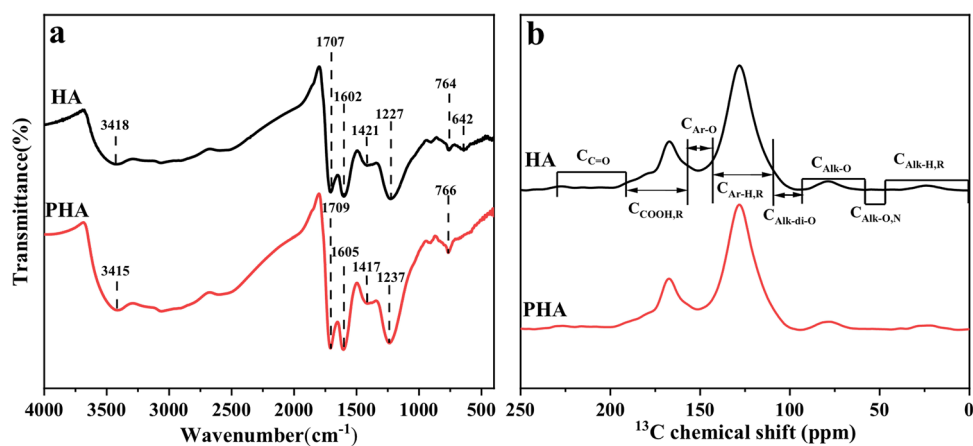


Figure 2. FTIR spectra (**a**) and ^{13}C NMR spectra (**b**) of HA and PHA.

C Type ppm	$\text{C}_{\text{Alk-H,R}} 0-45$	$\text{C}_{\text{Alk-O,N}} 45-60$	$\text{C}_{\text{Alk-O}} 60-91$	$\text{C}_{\text{Alk-di-O}} 91-110$	$\text{C}_{\text{Ar-H,R}} 110-142$	$\text{C}_{\text{Ar-O}} 142-156$	$\text{C}_{\text{COO-H,R}} 156-186$	$\text{C}_{\text{C=O}} 186-230$
HA	1.95	0.19	3.40	2.86	58.79	8.05	20.61	4.16
PHA	2.06	0.27	3.26	2.78	58.16	8.16	20.86	4.45

Table 2. Relative abundance of different carbon types (%) as determined by the ^{13}C RMN by CP/TOSS techniques for HA and PHA.

These FTIR spectra results suggested that during the preparation of HAP, the main functional groups of humic acid were not changed, while the relative content of carboxyl group increased.

HA and PHA had similar NMR spectra (Fig. 2b), and both of them had a high representation of aromatic C (58.79% for HA and 58.16% for PHA; Table 2), followed by carboxyl carbon (20.61% for HA and 20.86% for PHA). The relative content of carboxyl carbon in PHA was 1.2% higher than that in HA, which was consistent with the FTIR results in Table S1 (see Supplementary Table S1 online) but inconsistent with the results of

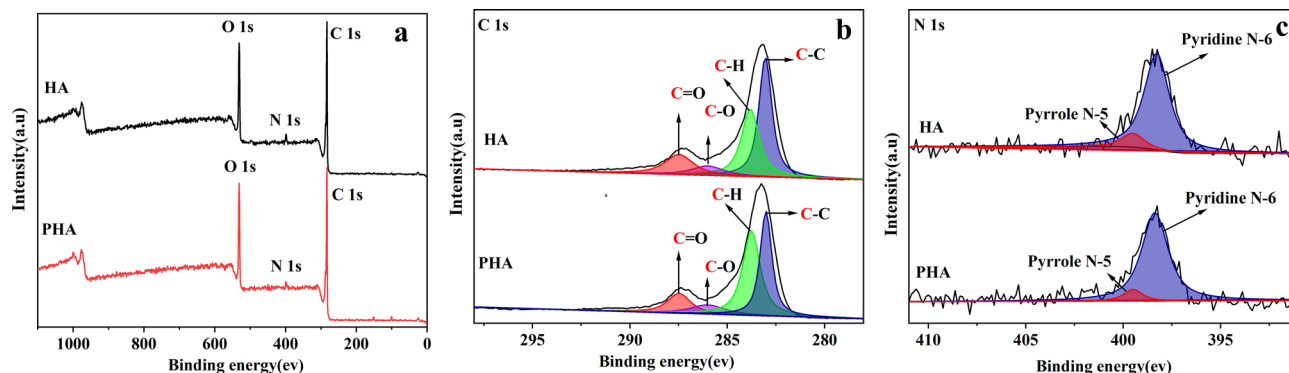


Figure 3. XPS spectra (a), C1s (b), and N1s (c) spectra of HA and PHA. Top: HA, bottom: PHA.

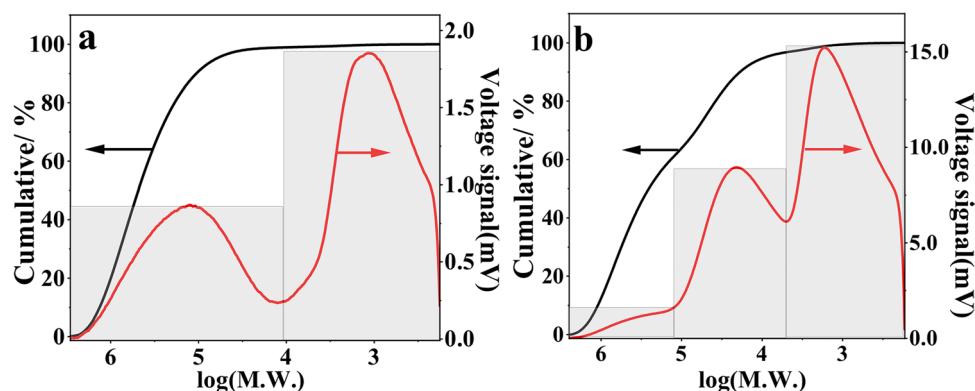


Figure 4. Molecular weight distribution curve of HA (a) and PHA (b).

Kolokassidou et al.²⁶, who reported that decarboxylation occurred at temperatures over 130 °C. This inconsistency occurred because in this study, the high temperatures caused by the reaction between phosphoric acid and potassium hydroxide was transient, while a slow increase in the temperature of the reaction system was needed when the decarboxylation reaction happened. In addition, the ratio of carboxyl group (the proportion of acidic functional groups) showed no significant difference between HA and PHA, but that of PHA7 was higher than that of HA7 (see Supplementary Table S2 online). This outcome suggested that PHA contained more carboxyl groups than HA, while parts of the groups in PHA were present in the form of carboxylate. The oxygen-containing and nitrogen-containing alkyl carbons in humic acid were hydrophilic carbons²⁵. We found that relative abundance of methoxy and N-alkyl carbons, O-alkyl carbons, and dioxide-alkyl carbon in HA was 6.45 (Table 2), while those carbon types of PHA was 6.31. This further indicated that PHA was less hydrophilic than HA.

XPS survey spectra confirmed the presence of C, N and O in both HA and PHA (Fig. 3a). Figure 3b shows the high-resolution C1s spectra of HA and PHA. The binding energy peaks centered at 283.04, 283.82, 286.00, and 287.50 eV for HA and at 283.01, 283.76, 286.00, and 287.48 eV for PHA are assignable to C–C, C–H, C–O, and C=O, respectively (see Supplementary Table S3 online)^{27–30}. Compared with HA, the relative amount of C–C in PHA decreased by 18.5%, while C–H increased by 29.6%, which indicated that the relative proportion of protonated C was higher than that of HA. Therefore, the long chains of humic acids were broken in the process of manufacturing HAP.

The peak in the N1s spectra of HA and PHA was assigned to Pyridine N-6 and Pyrrole N-5 (Fig. 3c)^{31–33}. The peak at 398.27 eV with 88.8% area of HA N1s spectra indicated the presence of pyridine N-6, and the peak at 399.50 eV with 11.2% area was attributed to pyrrole N-5. Compared with HA, PHA had more Pyridine N-6 (398.37 eV, 91.6%) and less Pyrrole N-5 (399.49 eV, 8.4%) (see Supplementary Table S4 online). This result was consistent with the result of the severely pyrolyzed chars (> 600 °C)³⁴.

O1s of X-ray photoelectron spectroscopy confirmed that PHA had more C=O as carboxyl (see Supplementary Fig. S1 and Table S5 online), in accordance with the FTIR (see Supplementary Table S1 online) and ¹³C NMR results (Fig. 2b, Table 2). In addition, the XPS spectra (Fig. 3a) and ³¹P NMR analysis (see Supplementary Fig. S2 online) confirmed the absence of P in PHA, which indicated that the humic acid and phosphate in HAP could be separated by adjusting the pH of the HAP solution.

Gel permeation chromatography was conducted to determine the molecular weight distribution of HA and PHA. According to the molecular weight distribution curve (Fig. 4a,b, Table 3), PHA had more components with small molecules than HA. HA had two groups, while PHA had three groups of different molecular weights. The two main molecular weight distribution areas of HA were 2.25×10^2 – 8.25×10^3 Da and 1.37×10^4 – 2.88×10^6 Da, accounting for 51.9% and 48.1% of all detected molecular weights, respectively. However, PHA had more small

Humic acids type	Main peaks (Da)	Interval M_w (Da)	Area (%)	Mw/Mn
HA	1.47×10^3	$2.25 \times 10^2 - 8.25 \times 10^3$	51.9	1.52
	1.26×10^5	$1.37 \times 10^4 - 2.88 \times 10^6$	48.1	2.60
PHA	1.67×10^3	$1.70 \times 10^2 - 4.92 \times 10^3$	61.4	2.00
	2.09×10^4	$5.03 \times 10^3 - 1.45 \times 10^5$	35.1	1.88
	1.51×10^5	$1.51 \times 10^5 - 2.89 \times 10^6$	3.5	1.45

Table 3. Molecular weight distribution of HA and PHA.

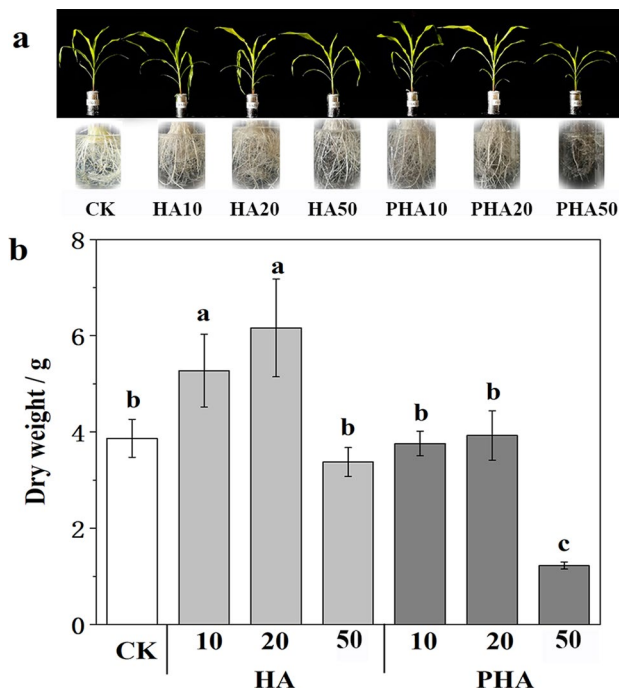


Figure 5. Growth status of ground and root of maize under different amounts of HA and PHA (a) and dry weight of maize with different amounts of HA and PHA (b). CK Hoagland's nutrient solution without humic acids, HA10, HA20, and HA50 Hoagland's nutrient solution with humic acids of 10, 20, and 50 mg C/L, PHA10, PHA20, and PHA50 Hoagland's nutrient solution with PHA of 10, 20, and 50 mg C/L. Bars represent mean \pm SD (n = 5). Means with no letter in common are significantly different ($P < 0.05$), as indicated by the Tukey's HSD test.

molecules, and the molecular weights ranged from $1.70 \times 10^2 - 4.92 \times 10^3$ Da accounting for 61.4% of all detected molecular weights. Therefore, during the preparation of humic acid enhanced phosphate fertilizer, some components of humic acid were decomposed to generate more small molecules.

Growth of the maize seedlings. HA stimulated maize seedling growth at low concentrations but inhibited growth at high concentrations, in accordance with the results from Chen et al.³⁵. However, the significant promoting effect has not been investigated when PHA is added at low concentrations, and PHA showed inhibition effects at high concentrations (Fig. 5b). Compared with CK, HA10 and HA20 (10 and 20 mg C/L) significantly increased the dry weight of plants by 36.2% and 59.2% ($P < 0.05$), respectively. There was no significant difference between the treatment with HA50 and CK ($P > 0.05$). However, PHA10 and PHA20 showed a similar stimulation with CK, and the dry weight with PHA50 was significantly lower than that with CK ($P < 0.05$). Under the same concentration, the dry weight under HA treatments was significantly higher than that of the PHA treatment ($P < 0.05$), so the growth promotion effect of PHA was inhibited compared with that of HA. This result indicated that the structural difference between HA and PHA affected their stimulating effect on plant growth, and combination with phosphate fertilizer may weakened the biological activity of humic acid.

Nutrients uptake of the maize seedlings. The N, P, and K uptake of maize increased and then decreased as the amount of added HA increased (Table 4). When the amount of added HA was 20 mg C/L, the uptake of N, P, and K in the maize was significantly higher than that of CK ($P < 0.05$). The effect of PHA in different amounts on plant nutrient absorption varied (Table 4). When the amount of added PHA was 10 and 20 mg C/L, the N

Treatment	N uptake (mg N plant ⁻¹)	P uptake (mg P plant ⁻¹)	K uptake (mg K plant ⁻¹)
CK	130.43 ± 5.23 ^c	34.75 ± 3.19 ^c	221.09 ± 4.18 ^{bc}
HA10	179.27 ± 9.64 ^b	47.90 ± 0.91 ^b	293.14 ± 3.71 ^a
HA20	206.78 ± 16.79 ^a	61.78 ± 2.73 ^a	298.68 ± 44.49 ^a
HA50	123.28 ± 7.54 ^c	36.74 ± 3.41 ^c	177.78 ± 5.17 ^c
PHA10	121.93 ± 1.86 ^c	45.59 ± 1.93 ^b	271.02 ± 4.48 ^{ab}
PHA20	121.78 ± 11.02 ^c	44.17 ± 1.99 ^b	240.45 ± 13.95 ^b
PHA50	45.28 ± 1.31 ^d	13.08 ± 0.96 ^d	82.45 ± 4.41 ^d

Table 4. Nitrogen (N), phosphorus (P) and potassium (K) uptake of the maize under different amounts of HA and PHA. CK Hoagland's nutrient solution without humic acids, HA10, HA20, and HA50 Hoagland's nutrient solution with humic acids of 10, 20, and 50 mg C/L, PHA10, PHA20 and PHA50 Hoagland's nutrient solution with PHA of 10, 20, and 50 mg C/L. Values are mean ± SD (n = 5), means with no letter in common are significantly different ($P < 0.05$), as indicated by the Tukey's HSD test.

uptake showed no significant difference with CK ($P > 0.05$), but it decreased for large amounts of added PHA. PHA and HA had similar effects on the P and K uptake: absorption was promoted at low concentrations and inhibited at high concentrations. However, for the same amount of added carbon, the P or K uptake of HA was higher than that of PHA. Therefore, PHA also had the function of promoting the absorption of P and K by plants, but its function was inhibited compared with that of HA, and the inhibitory effect became more obvious as the content of PHA increased.

Many studies have shown that the growth promotion effect of humic acids with small molecules was better than that with large molecules, and the better performance should also happen for humic acid with more carboxyl group^{36,37}. However, our research is likely to show an opposite result. This opposite result might be explained by the application amount of PHA. García et al.²² reported that humic acid with more reactive functional groups might promote root stimulation at lower concentrations, while that with recalcitrant structures requires higher concentrations to promote a similar stimulus. In this study, the best dosage of PHA for plant growth and nutrient uptake might even be lower than 10 mg C/L. Zhou et al.^{38,39} also reported that humic acid with a small molecular weight and a medium concentration (10 mg C/L) had the most promoting effect on maize plant growth, and when the amount of added humic acid is above 15 mg C/L, maize growth will be significantly inhibited. In addition, with further observation, we found that there were more humic acid materials attached to the root surface under the PHA treatments compared to the HA with the same carbon additions (Fig. 5a), which might be attributed to the hydrophilicity decrease of organics when the high temperature occurred during the preparation of phosphorus fertilizer²⁷. The attachments blocked the absorption channel of mineral nutrients in the root system, leading to the decrease of the nutrient uptake.

Conclusion

The high temperature, generated during the preparation process of humic acid enhanced phosphate fertilizer (HAP), cracked the structure of humic acid, and increased the relative amount of carboxyl groups and low molecular components. The hydrophobicity of PHA was also increased. Raw humic acid stimulated the maize seedlings growth and uptake of nitrogen, phosphorus and potassium. However, after combined with phosphate fertilizer, PHA showed a worse effect. This changed function might be attributed to the decreased hydrophilicity and unsuitable addition amount of PHA.

Methods

Preparation of materials. *Extraction of humic acid (HA) from weathered coal.* Humic acid (HA) was extracted from weathered coal (45°23' N, 119°15' E; Huolinhe, Tongliao, Inner Mongolia Autonomous Region, Northeast China) by a modified alkali extraction method, as described by Zhang et al.^{24,40}.

Manufacture of humic acid enhanced phosphate fertilizer (HAP). Humic acid enhanced phosphate fertilizer was prepared by simulating the production process of phosphate fertilizer in the laboratory, as shown in the flow chart in Fig. 6. A total of 42.64 parts by weight of potassium hydroxide (GR) was added into the mixture prepared by thoroughly mixing 20 parts by weight of HA with 37.36 parts by weight of phosphoric acid (GR). After continuous stirring, humic acid enhanced phosphate fertilizer was obtained.

Preparation of humic acid from HAP. HAP was dissolved in deionized water with a solid–liquid ratio of 1:10, and the solution pH was adjusted to 1.0 by 6 M HCl. After standing for 12 h, the solution was centrifuged to remove the soluble PO_4^{3-} , K^+ , and other ions, and the insoluble parts were collected as crude humic acid in HAP. Then, the crude humic acid in HAP was washed with deionized water at a solid–liquid ratio of 1:10 three times and oven-dried at 50 °C to obtain the final humic acid in HAP (PHA). A schematic diagram of the preparation of humic acid from HAP is shown in Fig. 6.

Characterization of HA and PHA. *Elemental analyses.* The C, N, H, and S contents of HA and PHA were determined using an element analyzer (Vario Micro Cube, Elementar Analysensysteme GmbH, Germany),

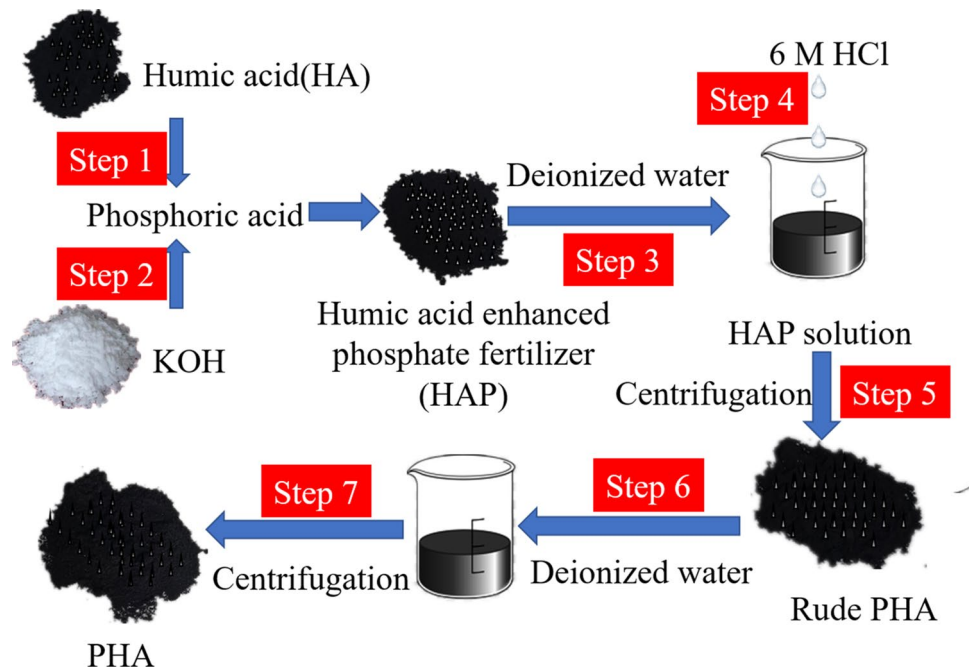


Figure 6. Preparation of humic acid extracted from humic acid enhanced phosphate fertilizer (PHA).

and the ash content was determined by burning in a muffle furnace. The oxygen content was calculated by subtracting.

Carboxylic groups and phenolic hydroxyl groups. The contents of the carboxylic groups and phenolic hydroxyl groups of HA and PHA were determined by the methods described by Klavins et al. and Zhang et al.^{24,41}. To reduce the difference in the carboxylate contents in HA and PHA on the comparison of the carboxylic acid content, the pH of the HA and PHA was adjusted to 7.0, and then their acidic functional groups were compared. The adjustment of the pH was conducted according to the following process: 10 g of HA or PHA was mixed into 100 mL of deionized water, and then the pH of the HA and PHA solution was adjusted to 7.0 with 5 M NaOH. After centrifugation and freeze drying, the processed samples were obtained and named as HA7 and PHA7, respectively.

Fourier transform infrared spectroscopy. The atom group information of the HA and PHA was determined by a Fourier transform infrared spectrophotometer (Nicolet iS10, Thermo Nicolet Corporation, America). Infrared spectra (IR) were recorded in the 4000–400 cm^{-1} region using the KBr pellet method²⁴. The baseline correction and data smoothing correction of the spectra were conducted with the OMINC 8.2 software. The main peak area was integrated to calculate the relative absorption intensity of each functional group using the Origin 9.0 software.

Scanning electron microscopy. The morphology of the HA and PHA was examined using a scanning electron microscope (SU8020, Hitachi, Japan).

X-ray photoelectron spectroscopy. X-ray photoelectron spectroscopic measurement (XPS, PHI QUANTERA-II SXM system, Japan/Uivac-PHI, INC) was used to obtain information about the surface element composition, chemical state, molecular structure and chemical bonds of the HA and PHA. An Al K α ray was used as the excitation source, and the energy was 1486.6 eV. The XPS spectra were analyzed by the XPSPEAK software.

Solid-state ^{13}C -nuclear magnetic resonance spectroscopy. To clarify the detailed distribution of the carbon functional groups of the HA and PHA, a solid-state ^{13}C nuclear magnetic resonance spectrometer (Bruker AVANCE III HD 400 MHz, Switzerland) was used. The NMR measurement was carried out with the following parameters: H/X dual resonance solid probe, 4 mm ZrO_2 rotor, speed of spinning: 5 kHz, ^{13}C detection resonance frequency: 100.625 MHz, sampling time: 5.12 μs , spectral width: 100 kHz, 90° pulse-length: 4 μs , recycle delay time: 5.47 μs , number of scans: 4096 times, and chemical shift calibrated with standard glycine. Baseline correction and spectra integration were conducted using the MestReNova 9.0 software. The carbon types were divided into Alkyl carbons ($\text{C}_{\text{Alk-H,R}}$, 0–45 ppm), methoxy and N-alkyl carbons ($\text{C}_{\text{Alk-O,N}}$, 45–60 ppm), O-alkyl carbons ($\text{C}_{\text{Alk-O}}$, 60–91 ppm), dioxide-alkyl carbon ($\text{C}_{\text{Alk-di-O}}$, 91–110 ppm), aromatic carbon ($\text{C}_{\text{Ar-H,R}}$, 110–142 ppm), O-aromatic carbon ($\text{C}_{\text{Ar-O}}$, 142–156 ppm), carboxyl carbon ($\text{C}_{\text{COO-H,R}}$, 156–186 ppm), and carbonyl carbon ($\text{C}_{\text{C=O}}$, 186–230 ppm)^{22,42}.

Gel permeation chromatography. The molecular weight distributions of the HA and PHA was determined by gel permeation chromatography (GPC, Shimadzu LC-20A, Japan). The instrument configuration was as follows: LC20 high-performance liquid chromatography pump (Shimadzu, Japan), RID-20A refractive index detector (Shimadzu, Japan), TSKgel GMPWXL water phase gel chromatography column (TOSOH, Japan), Rheodyne 7725i manual six-port valve sampler (20 μ l loop, USA), and HW-2000 GPC chromatography workstation. Polyethylene glycol samples were used as standard substances. HA or PHA (100 mg) was dissolved in 10 mL of a 0.1 M NaOH solution and then filtered through a 0.22 μ m membrane filter before determination. The operation parameters were as follows: 35 °C column temperature, 0.1 N NaNO₃ and 0.06% NaN₃ aqueous solution as mobile phase, and 0.6 mL/min flow rate.

Plant materials and incubation conditions. Hydroponic experiments were conducted in an environmentally controlled greenhouse (16/8 h light/dark cycle, 300 μ mol m⁻² s⁻¹ light intensity, 28/21 °C temperature, 70% relative humidity) at the Dezhou experimental station, Chinese Academy of Agricultural Sciences, Shandong, China. Maize (*Zea mays* L. cv ZD 958) seeds were surface sterilized with a 0.1% NaClO solution for 10 min, washed 3 times with distilled water, and immersed in distilled water for 4 h. Then, the seeds were placed on moistened filter paper at 25 °C in the dark for 4 days until germination. After the endosperm was moved, the seedlings were transplanted to culture containers filled with Hoagland nutrient solution (5.0 mM Ca(NO₃)₂; 5.0 mM KNO₃; 2.0 mM MgSO₄; 1.0 mM KH₂PO₄; 45 μ M H₂BO₃; 10 μ M MnCl₂; 0.8 μ M ZnSO₄; 0.3 μ M CuSO₄; 0.4 μ M Na₂MoO₄; 0.02 μ M EDTA-Fe) with HA or PHA^{39,43}. The added amounts of HA and PHA were 0, 10, 20, and 50 mg C/L, code named CK, HA10 or PHA10, HA20 or PHA20, HA50 or PHA50, respectively. Each treatment was repeated five times. The pH of the nutrient solutions was adjusted to 6.1, and they were renewed every 72 h. The entire hydroponic experiment lasted for 30 days, and then the plants were harvested.

Sampling and laboratory analyses. The harvested plant was divided into roots, stalks and leaves, and each part was washed with distilled water, drained with blotting paper, and weighed to obtain the fresh weight. Subsequently, they were oven-dried at 105 °C for 30 min and at 65 °C to constant weight and weighed to obtain the dry weight. The dried samples were ground for N, P, and K analyses. After wet digestion with H₂SO₄-H₂O₂, the N, P, and K concentrations in the maize plant were determined by using a Kjeldahl apparatus (KDY-9820, Beijing Tongrunyuan Electromechanical Technology Co. Ltd., China), UV-vis spectrometer (UV-5500PC, Shanghai Precision Instruments Co., Ltd., China), and flame photometer (FP6400, Shanghai Jinpeng Analytical Instrument Co. Ltd., China), respectively⁴⁴.

Calculations and statistical analyses. The difference between the HA and the PHA in the elemental composition was compared by analysis of variance (ANOVA, SAS 9.1, SAS Institute Inc., NC, USA) with the least significant difference (LSD) test ($\alpha=0.05$). The differences between HA and PHA with different addition amount on plant growth stimulation were compared with the Tukey's HSD test ($\alpha=0.05$). Graphs were compiled using the Origin 9.0 software.

Received: 2 May 2020; Accepted: 10 September 2020

Published online: 15 October 2020

References

- Hayes, M. H. B. & Wilson, W. S. *Humic Substances, Peats and Sludges* (Royal Society of Chemistry, London, 1997).
- Du, Z. Y. *et al.* Movement of phosphorus in a calcareous soil as affected by humic acid. *Pedosphere* **23**, 229–235 (2013).
- Yang, F. *et al.* Synthetic humic acids solubilize otherwise insoluble phosphates to improve soil fertility. *Angew. Chem. Int. Edit.* **58**, 18813–18816 (2019).
- Dobbss, L. B. *et al.* Changes in root development of arabidopsis promoted by organic matter from oxisols. *Ann. Appl. Biol.* **151**, 199–211 (2007).
- Xu, W., Shi, W., Jia, L., Liang, J. & Zhang, J. Tft6 and Tft7, two different members of tomato 14-3-3 gene family, play distinct roles in plant adaption to low phosphorus stress. *Plant Cell. Environ.* **35**, 1393–1406 (2012).
- Azevedo, I. G., Olivares, F. L., Ramos, A. C., Bertolazi, A. A. & Canellas, L. P. Humic acids and Herbaspirillum seropedicae change the extracellular H⁺ flux and gene expression in maize roots seedlings. *Chem. Biol. Technol. Ag.* **6**, 8 (2019).
- Li, Z. *et al.* Effects of value-added phosphate fertilizers on yield and phosphorus utilization of winter wheat. *Plant Nutr. Fert. Sci.* **19**, 1329–1336 (2013).
- Li, Z. *et al.* Effects of value-added phosphate fertilizers on transformation of inorganic phosphorus in calcareous soils. *Plant Nutr. Fert. Sci.* **19**, 1183–1191 (2013).
- Li, J. *et al.* Effect of adding humic acid to phosphorous fertilizer on maize yield and phosphorus uptake and soil available phosphorus conten. *Plant Nutr. Fert. Sci.* **23**, 641–648 (2017).
- Ma, M. K., Yuan, L., Li, Y. T., Gao, Q. & Zhao, B. Q. The effect of sulfonated humus acid phosphate fertilizer on enhancing grain yield and phosphorus uptake and utilization in winter wheat. *Plant Nutr. Fert. Sci.* **25**, 362–369 (2019).
- Du, O., Zhang, S., Antonietti, M. & Yang, F. Sustainable leaching process of phosphates from animal bones to alleviate the world phosphate crisis. *ACS Sustain. Chem. Eng.* **8**, 9775–9782 (2020).
- Yang, F. & Antonietti, M. Artificial humic acids: sustainable materials against climate change. *Adv. Sci.* **7**, 1902992 (2020).
- Zhang, S., Du, Q., Cheng, K., Antonietti, M. & Yang, F. Efficient phosphorus recycling and heavy metal removal from wastewater sludge by a novel hydrothermal humification-technique. *Chem. Eng. J.* **394**, 124832 (2020).
- Yang, F. & Antonietti, M. The sleeping giant: a polymer view on humic matter in synthesis and applications. *Prog. Polym. Sci.* **100**, 101182 (2020).
- Zhang, Y. C., Dong, Z. Y., Zhao, Y. C., Yang, M. & Chen, G. W. Preparation of monoammonium phosphate by autothermal crystallization in a microreactor. *Chem. React. Eng. Technol.* **32**, 392–399 (2016).

16. Peng, B. L. & Xiang, S. L. Study on industrial technology of fertilizer grade wet-process phosphoric acid to produce industrial MAP. *Mod. Chem. Ind.* **37**, 152–155 (2017).
17. Long, L. J., Wang, L. A., Yu, C. L., Wei, X. Y. & Zhuo, L. Characterization of modified sludge-based humic acid and its adsorption properties for Cu²⁺. *China Environ. Sci.* **37**, 1016–1023 (2017).
18. Zhang, X. W. *et al.* Effects of different corn straw amendments on humus composition and structural characteristics of humic acid in black soil. *Commun. Soil. Sci. Plan* **51**, 107–117 (2020).
19. Zhou, L. P., Yuan, L., Zhao, B. Q., Li, Y. T. & Lin, Z. A. Structural characteristics of humic acids derived from Chinese weathered coal under different oxidizing conditions. *PLoS ONE* **14**, e0217469 (2019).
20. Zhou, L. P. *Structure of humic acids oxidized by hydrogen peroxide and its regulation on maize roots* (Chinese Academy of Agricultural Sciences, Beijing, 2019).
21. Jindo, K. *et al.* Root growth promotion by humic acids from composted and non-composted urban organic wastes. *Plant. Soil* **353**, 209–220 (2012).
22. Garcia, A. C. *et al.* Structure-property-function relationship in humic substances to explain the biological activity in plants. *Sci. Rep.* **6**, 20798 (2016).
23. Albuzio, A., Ferrari, G. & Nardi, S. Effects of humic substances on nitrate uptake and assimilation in barley seedlings. *Can. J. Soil. Sci.* **66**, 731–736 (1986).
24. Zhang, S. Q. *et al.* Characterization of pH-fractionated humic acids derived from Chinese weathered coal. *Chemosphere* **166**, 334–342 (2017).
25. Li, S. Z. & Zhu, S. Q. Relationship between surface hydrophobicity and composition of coal. *Clean Coal Technol.* **10**, 15–18 (2004).
26. Kolokassidou, C., Pashalidis, I., Costa, C. N., Efstathiou, A. M. & Buckau, G. Thermal stability of solid and aqueous solutions of humic acid. *Thermochim. Acta.* **454**, 78–83 (2007).
27. Wang, C. *et al.* Insights into the roles of the morphological carbon structure and ash in the sorption of aromatic compounds to wood-derived biochars. *Sci. Total. Environ.* **693**, 133455 (2019).
28. Li, X. W. *et al.* Molecular characteristics of the refractory organic matter in the anaerobic and aerobic digestates of sewage sludge. *RSC Adv.* **8**, 33138–33148 (2018).
29. Li, W. Q. *et al.* Linking lignin source with structural and electrochemical properties of lignin-derived carbon materials. *RSC Adv.* **8**, 38721–38732 (2018).
30. Yang, Z. B., Feng, S. L., Yao, W., Han, J. G. & Wang, H. B. Synthesis of novel rambutan-like graphene@aluminum composite spheres and non-destructive terahertz characterization. *RSC Adv.* **9**, 3486–3492 (2019).
31. Doskočil, L., Burdíkóvá-Szewieczková, J., Enev, V., Kalina, L. & Wasserbauer, J. Spectral characterization and comparison of humic acids isolated from some European lignites. *Fuel* **213**, 123–132 (2018).
32. Bo, W. U., Hao-Quan, H. U., Zhao, Y. P., Jin, L. J. & Fang, Y. M. XPS analysis and combustibility of residues from two coals extraction with sub- and supercritical water. *J. Fuel Chem. Technol.* **37**, 385–392 (2009).
33. Rabchinskii, M. K. *et al.* From graphene oxide towards aminated graphene: Facile synthesis, its structure and electronic properties. *Sci. Rep.* **10**, 6902 (2020).
34. Kelemen, S. R. *et al.* Nitrogen transformations in coal during pyrolysis. *Energ. Fuel.* **12**, 159–173 (1998).
35. Chen, Y. & Solovitch, T. Effects of humic substances on plant growth. *Acta Hort. Sin.* **221**, 412–412 (1988).
36. Rose, M. T. *et al.* Chapter two—a meta-analysis and review of plant-growth response to humic substances: Practical implications for agriculture. *Adv. Agron.* **124**, 37–89 (2014).
37. Eyheraguibel, B., Silvestre, J. & Morard, P. Effects of humic substances derived from organic waste enhancement on the growth and mineral nutrition of maize. *Bioresour. Technol.* **99**, 4206–4212 (2008).
38. Zhou, L. P., Yuan, L., Zhao, B. Q., Li, Y. T. & Lin, Z. A. Contents of the main metabolites in maize affected by humic acids with different molecular weight derived from weathered coal. *Plant Nutr. Fert. Sci.* **25**, 142–148 (2019).
39. Zhou, L. P., Yuan, L., Zhao, B. Q., Li, Y. T. & Lin, Z. A. Response of maize roots to different additive amounts of weathered coal humic acids. *Sci. Agric. Sin.* **52**, 285–292 (2019).
40. Stevenson, F. J. *Humus chemistry: Genesis, composition, reactions* (John Wiley & Sons Inc, New York, 1994).
41. Klavins, M. & Purmalis, O. J. H. A. Properties and structure of raised bog peat humic acids. *J. Mol. Struct.* **1050**, 103–113 (2013).
42. Mao, J. D., Olk, D. C., Fang, X. W., He, Z. Q. & Schmidt-Rohr, K. Influence of animal manure application on the chemical structures of soil organic matter as investigated by advanced solid-state NMR and FT-IR spectroscopy. *Geoderma* **146**, 353–362 (2008).
43. Mao, D. R. & Shen, J. B. *Research Methods of Plant Nutrition* (China Agricultural University Press, Beijing, 2011).
44. Kalra, Y. P. Handbook of reference methods for plant analysis. *Crop Sci.* **38**, 1710–1711 (1998).

Acknowledgements

This work was financially supported by the National Key Technologies R&D Program of China during the 13th Five-Year Plan period (2016YFD0200402).

Author contributions

B.Q.Z. and L.Y. designed the experiments. J.Y.J. performed the experiments. J.Y.J. and S.Q.Z. wrote the main manuscript. Q.Z.X. contributed to the structural analysis of the materials. L.Y., Y.T.L. and Z.A.L. contributed to data interpretation. All authors discussed the results and commented on the manuscript at all stages.

Competing interests

The authors declare no competing interests.

Additional information

Supplementary information is available for this paper at <https://doi.org/10.1038/s41598-020-74349-6>.

Correspondence and requests for materials should be addressed to B.Z.

Reprints and permissions information is available at www.nature.com/reprints.

Publisher's note Springer Nature remains neutral with regard to jurisdictional claims in published maps and institutional affiliations.



Open Access This article is licensed under a Creative Commons Attribution 4.0 International License, which permits use, sharing, adaptation, distribution and reproduction in any medium or format, as long as you give appropriate credit to the original author(s) and the source, provide a link to the Creative Commons licence, and indicate if changes were made. The images or other third party material in this article are included in the article's Creative Commons licence, unless indicated otherwise in a credit line to the material. If material is not included in the article's Creative Commons licence and your intended use is not permitted by statutory regulation or exceeds the permitted use, you will need to obtain permission directly from the copyright holder. To view a copy of this licence, visit <http://creativecommons.org/licenses/by/4.0/>.

© The Author(s) 2020